Change detection for semi-automatic map database updating

Allan Aasbjerg Nielsen and Brian Pilemann Olsen

DTU Space
National Space Institute

Contents

1 Foreword

This report is the fulfilment for 2009 of "Ydelsesaftale mellem Kort & Matrikelstyrelsen og Institut for Rumforskning og -teknologi, DTU om myndigsbetjening af Kort & Matrikelstyrelsen i form af forskningsbaseret rådgivning og forskning i relation til geodæsi og kortlægning i 2009-2012", "Resultatmål 3: Metodeudvikling til topografisk kortlægning, Krav 1".

The report has been created as a result of a co-operation between the Technical University of Denmark (DTU), Department DTU Space and the National Survey and Cadastre – Denmark (KMS), Department Topographic Mapping. The KMS has defined the problem and delivered data for solving the problem and DTU has developed the solution.

The problem dealt with in this report concerns automatic change detection: determination of changes in-between two states.

KMS conducts flight campaigns over a given geographical area approximately every third year (sometimes even more often). The outcome is nadir looking aerial photos and computed ortho photos. The photos are georeferenced by GPS, INS and aerial triangulation, and the images are used for 3D mapping.

At time T_0 the map database, at this time FOT, is established. At time $T_0 + \Delta t$ the map data base is to be revised, and a new flight campaign carried out. The revision process is carried out by 3D-superimposition of the existing map database onto the stereo models from the new flight campaign.

Differences (changes) are manually detected and collected by a human stereo operator. This is a process step that is very time consuming and thus costly. Also it is not evident if all changes are detected by the human operator. For these reasons the development of an automatic change detection algorithm would be very profitable as map production costs could be reduced dramatically. If all changes changes are detected automatically the human stereo operator could automatically "'jump'" from one potential change to another only using time collecting the change and *not* wasting time searching for changes.

This report presents a new method for automatic change detection. The algorithm is based on an iterated version of an established method in multivariate statistics, namely canonical correlation analysis. The algorithm has been applied to a representative Danish suburban test area of 1x1 km^2 and the outcome of this investigation is presented.

Contact information:

Allan Aasbjerg Nielsen
aa@space.dtu.dk

Poul Frederiksen (KMS)
pof@kms.dk

Brian Pilemann Olsen (KMS)
bpo@kms.dk

2 Introduction

In almost all areas of our society today, topographic data and geo-spatial map databases play a major role. This is valid on a global as well as on a local level. Monitoring pollution and changes of climate are examples of applications where worldwide geo-spatial data is required. At a local level there is an increased demand on up-to-date information for planning and decision-making.

A map database is only a snapshot or a status of the landscape or area it represents. As the landscape changes over time due to e.g. construction work, the maps describing the area gets outdated corresponding to the degree of change, and as time goes by the database slowly degenerates and gets more and more untrustworthy.

Updating geo-spatial map databases to reflect continuous changes is a major task, which has previously been carried out either as a full manual re-mapping of the total area in question or by updating the existing database. Both methods are time consuming and labour-intensive and therefore costly.

Today national geo-spatial map databases have an update cycle of 3 to 5 years. For most purposes, a 3 to 5 years update cycle is not sufficient, and therefore the urge for new, more efficient and cost effective revision methods is growing.

The process of updating an existing map database can be divided into 3 steps:

1. Change detection

2. Classification of the changes detected

3. Finally registration and updating of the database

Change detection and classification of changes are the most complicated and expensive tasks of the updating procedure, and thus much can be saved if these can can be more or less automated.

This report deals with the problem of automating the change detection step in the revision process, especially looking for changes in the building layer.

3 Related work

Many research organisations have in past years spent time and effort trying to develop methods that could automate or ease the change detection process.

Baltsavias (Baltsavias, 2004) gives a thorough overview.

Skriver et al (Skriver et al., 2000) investigate how airborne Synthetic Aperture Radar (SAR) data can be used for topographical mapping.

Knudsen and Olsen (Knudsen and Olsen, 2003; Olsen, 2004; Olsen et al., 2002) have described algorithms for change detection based on pixel-wise classification comparing digital aerial images to existing vector database. The main focus is on detecting changes in the building layer.

The non-profit organisation EuroSDR (http://www.eurosdr.net) has hosted numerous projects concerning change detection:

- Detection of Unregistered Buildings for Updating 2D Databases (EuroSDR, 2009)

- Evaluation of Building Extraction (EuroSDR, 2006)

- Change Detection (EuroSDR, 2006)

- Automated Extraction, Refinement, and Update of Road Databases from Imagery and Other Data (EuroSDR, 2006)

4 Methods

Change over time between two multispectral images is here detected by means of the IR-MAD method ([Canty and Nielsen](#), 2008; [Nielsen](#), 2007). This method builds on an iterated version of an established method in multivariate statistics, namely canonical correlation analysis, see below for details. It finds orthogonal (i.e., uncorrelated) linear combinations of the multivariate data at two time points that have maximal correlation. These linear combinations are called the canonical variates (CV) and the corresponding correlations are called the canonical correlations. There is one set of CVs for each time point. The difference between the two set of CVs represent the change between the two time points and are called the MAD variates or the MADs for short. MAD is an acronym for multivariate alteration detection. (Alteration here means change and has nothing to do with for example hydrothermal alteration known from geology.)

The sum of the squared MAD variates (properly normed to unit variance) gives us change variables that will ideally follow a chi-squared (χ^2) distribution with p degrees of freedom for the no-change pixels; p is the number of spectral bands in the image data. This image is called the "change image" below. The chi-squared image is the basis for calculating an image of probability for no-change, i.e., the probability for finding a higher value of the chi-squared statistic than the one actually found. This image is the weight image in the iteration scheme mentioned above. Iterations stop when the canonical correlations stop changing.

If the chi-squared image is thresholded at a very high percentile in the chi-squared distribution we obtain a binary change image where change is indicated by the colour white. If we use the opening operation from mathematical morphology on this image, we obtain a binary change image where the colour white indicates significant change in large objects. This image is called the "significant change image" below. The sizes of the objects thus detected depend on the size of the structuring element applied in the opening process.

4.1 Canonical Correlation Analysis, CCA

Consider first two p-band multispectral images of the same scene acquired at different times, between which acquisitions ground reflectance changes have occurred at some locations, but not everywhere. Assume without loss of generality that both images have pixel intensities with zero mean. Representing observations (pixel intensities) in the first multispectral image by a random vector $X = [X_1 \ldots X_p]^T$, we can make a linear combination of the intensities for all spectral bands, creating a scalar image characterized by the random variable $U = a^T X$. The vector of coefficients a is as yet unspecified. We do the same for the second image, represented by Y, forming the linear combination $V = b^T Y$, and then look at the scalar difference image $U - V$. This combines all of the change information into a single image, but one of course still must choose the coefficients a and b in some suitable way. In ([Nielsen et al.](#), 1998) it is suggested that they be determined by applying standard Canonical Correlation Analysis (CCA), first described by Hotelling in 1936, to the images X and Y. This leads to the coupled generalized eigenvalue problems

$$\Sigma_{12}\Sigma_{22}^{-1}\Sigma_{21}a = \rho^2\Sigma_{11}a \tag{1}$$

$$\Sigma_{21}\Sigma_{11}^{-1}\Sigma_{12}b = \rho^2\Sigma_{22}b \tag{2}$$

where Σ_{11} and Σ_{22} are the variance-covariance matrices of the two images and $\Sigma_{12} = \Sigma_{21}^T$ is the inter-image covariance matrix. Solution of the eigenvalue problems generates new multispectral images $U = [U_1 \ldots U_p]^T$ and $V = [V_1 \ldots V_p]^T$, the components of which are called the canonical variates (CVs). The CVs are ordered by similarity (correlation) rather than, as in the original images, by wavelength. The canonical correlations $\rho_i = \text{corr}(U_i, V_i), i = 1, \ldots, p$, are the square roots of the eigenvalues of the coupled eigenvalue problem and a_i and $b_i, i = 1, \ldots, p$, which determine U and V from X and Y, are the eigenvectors. The pair U_1, V_1 is maximally correlated, the pair (U_2, V_2) is maximally correlated subject to being orthogonal to (uncorrelated with) both U_1 and V_1, and so on.

4.2 Multivariate Alteration Detection, MAD

Performing paired differences (in reverse order) then generates a sequence of transformed difference images

$$M_i = U_{p-i+1} - V_{p-i+1}, \ i = 1, \ldots, p, \tag{3}$$

referred to as the MAD variates or the MADs, having nice statistical properties which make them very useful for visualizing and analyzing change information. Thus for instance they are uncorrelated,

$$\text{cov}(M_i, M_j) = 0, \ i \neq j, \tag{4}$$

and have, by virtue of our chosen ordering, successively decreasing variances given by

$$\text{var}(M_i) = \sigma_{M_i}^2 = 2(1 - \rho_{p-i+1}). \tag{5}$$

The fact that several additions and subtractions go into determining the MAD variates means that, from the Central Limit Theorem, they are ideally normally distributed. The usefulness of the MAD variates for automatic radiometric normalization stems from the fact that they are invariant under affine transformations of either or both of the original images.

4.2.1 Iterated MAD

Now consider two images of a scene, acquired at different times under similar illumination conditions, but for which no ground reflectance changes have occurred whatsoever. Then the only differences between them will be due to random effects like instrument noise and atmospheric fluctuation. In such a case we would expect that the histogram of any difference component that we generate would be very nearly Gaussian. In particular, the MAD variates, being uncorrelated, should follow a multivariate normal distribution with diagonal covariance matrix. The MAD variates associated with change observations will deviate more or less strongly from such a multivariate normal distribution. Therefore, in the presence of genuine change, we expect an improvement of the sensitivity of the MAD transformation if we place emphasis on establishing an increasingly better background of no change against which to detect change. This can be done in an iteration scheme in which observations are weighted by the probability of no change, as determined on the preceding iteration, when estimating the sample means and covariance matrices which determine – via CCA – the MAD variates for the next iteration. The probability weights may be obtained by examining the MAD variates directly. Let the random variable Z represent the sum of the squares of the standardized MAD variates

$$Z = \sum_{i=1}^{p} \left(\frac{M_i}{\sigma_{M_i}} \right)^2, \tag{6}$$

where σ_{M_i} is given by Equation 5. Then, since the no-change observations are normally distributed and uncorrelated, their realizations should be chi-square distributed with p degrees of freedom (distribution function $P_{\chi^2;p}(z)$). For each iteration, the observations z (realizations of the random variable Z) can then be given weights determined by the chi-square distribution, namely

$$\Pr(\text{no change}) = 1 - P_{\chi^2;p}(z). \tag{7}$$

Pr(no change) is the probability that a sample z drawn from the chi-squared distribution could be that large or larger. A small z implies a large probability of no change. Other weighting schemes are possible, for instance using unsupervised classification of change/no-change observations. Iteration of the MAD transformation will continue until some stopping criterion is met, such as lack of change in the canonical correlations ρ_i, $i = 1, \ldots, p$.

5 Data

Kort & Matrikelstyrelsen (KMS) has delivered to Institut for Rumforskning og -teknologi, DTU (DTU Space) data in the form of 25 orthophotos consisting of 1 km by 1 km 10 cm pixels. Each of the 25 images is 10,000 by 10,000 pixels, 8 bit in each of the colours red, green and blue. Data exist from 2007, 2008 and 2009 in ECW and TIFF formats.

Of the data delivered by KMS we concentrate on the 1 km by 1km square termed 6168_726. We note that the 2007 and the 2009 data are acquired before foliation, the 2008 data after. Also, judged visually, the parallax differences seem smaller between the 2007 and the 2009 data than between the other possible time point pairs. This makes the 2007 and 2009 data the best for an initial study. Work is done on the uncompressed TIFF data only.

6 Results

Each of the 25 datasets takes up 300 MB of space. An implementation of the IR-MAD method in ENVI/IDL (Canty, 2010) allows for practically any-size-images. Each iteration takes just over 5 minutes on a 32 bit, 2.00 GHz Intel Core 2 CPU laptop with 2.50 Gbyte, 998 MHz memory, typically around 15 iterations are needed.

The float chi squared image (the "change image") output from IR-MAD was stored in byte format stretched linearly from 16.269 (the 99.9% percentile of the corresponding no-change distribution) and 1,000 (a somewhat arbitrary choice). The threshold in this byte image was found automatically in Matlab by means of the graythresh command. Following this the opening was done by means of Matlab command imopen with a disk shaped structuring element with radius 10 to obtain the "significant change image".

Figure 1 illustrates results from change analysis of the 6168_726 square on time point pairs 2007/2009. Upper left panel shows the full 10,000 by 10,000 scene for the first time point (2007). Upper right panel shows the full 10,000 by 10,000 scene for the second time point (2009). Lower left panel shows the full 10,000 by 10,000 scene chi-squared, i.e., the "change image". Finally the lower right panel shows the full 10,000 by 10,000 scene chi-squared image thresholded and opened, i.e., the "significant change image".

As can be seen from figure 1, all significant changes have been detected.

Figure 2 shows a closeup of the area marked by a red square in the lower left corner of each panel in figure 1. Upper left panels shows the zoomed area for the first time point. Upper right panel shows the zoomed area for the second time point. The lower left panel shows the zoomed area for the for chi-squared, i.e., the "change image". Finally the lower left panel shows the zoomed area for the chi-squared image thresholded and opened, i.e., the "significant change image".

Taking a closer look at the significant change map (LR panel) in figure 2, it can be realised that the two new buildings have been detected, but it can also be seen that the detections are not perfect. Additionally a car has been pointed out as "new", and some containers depicted as removed.

Further results can be found in appendix A to C

Appendix A shows nine additional examples taken from various positions in the time point pairs 2007/2009. Appendix B shows examples of registration problems between time point pairs 2007/2008. Appendix C shows examples of registration problems between 2008/2009.

7 Conclusions

Generally the method seems to give few false positives (i.e., indications of change where actual change does not occur) and false negatives (the opposite, i.e., no indication of change where change actually does occur). A false positive is sometimes termed a type I error, a false alarm or an α error. A false negative is sometimes termed a type II error or a β error.
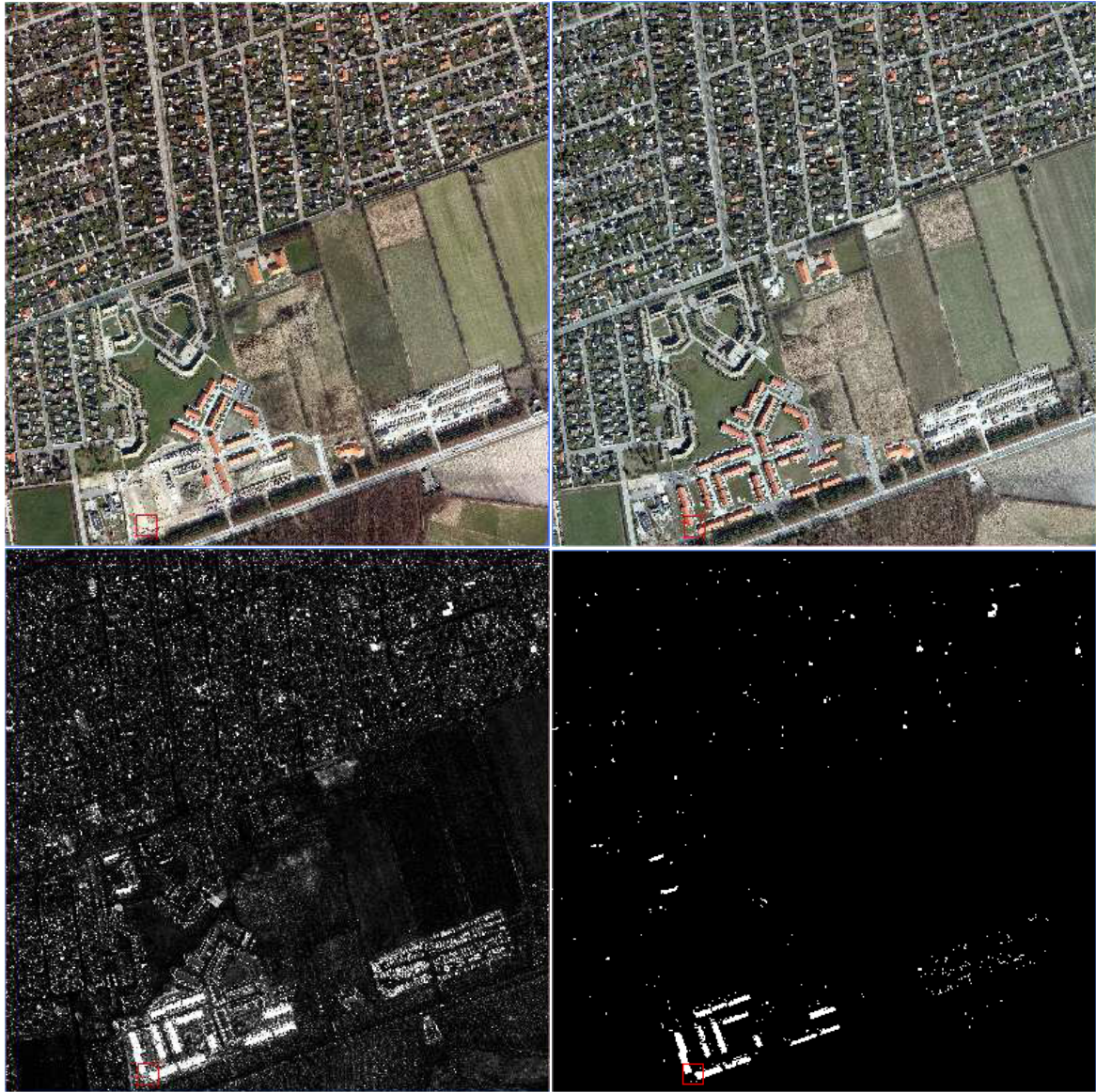
Figure 1: Results for 6168_726. Changes between years 2007 and 2009. UL: Full scene 2007. UR: Full scene 2009. LL: Change image. LR: Significant change image

We see that the main problem, when it comes to false alarms, is due to mis-registrations caused by the fact that the orthophotos are produced based on a terrain model and not a surface model. Better results for change detection would therefore be obtained by working on *true* orthophotos rather than orthophotos, i.e., orthophotos that are produced in a process which allows not only for the terrain model but for the surface model including buildings.

A change from for example bare soil to a new building with a soil coloured roof (or vice versa) is likely to be missed, i.e., produce false negatives. This could be handled by including height data. The largest radiometric changes are related to the presence and absence of water (typically seen in swimming pools being empty or full).

Specular reflection (mirroring) due to unfortunate geometry of the illumination source (the sun) relative to the sensor at one of the two time points gives rise to false positives. The presence or absence of large cars, containers, campers etc. at one of the two time points gives rise to false positives (when the goal is to find changes in what is to become the building theme of a map vector database).

Figure 2: Results for the zoomed area from 6168_726. Changes between years 2007 and 2009. UL: Zoomed area from the 2007 scene. UR: Zoomed area from the 2009 scene. LL: Change image. LR: Significant change image

7.1 Future work

Future work could wisely include:

1. work on *true* orthophotos,

2. more thorough investigations of the change detected, i.e., the number of and nature of false positives and false negatives,

3. experiments on the threshold applied in the chi-squared image,

4. experiments on the size of the structuring element in the opening,

5. attempts to establish a typical variance-covariance structure for two consecutive years pre-foliation airborne 10 cm 3, 4 or 5 band image data. If this can be done, all we need to store is the eigen vectors and the correlations after iterations for a representative time point pair and use those for all future time

point pairs. This would give an enormous speed-up (from the present just over 5 minutes per iteration, 15 iterations, to the time it takes to do the projections and calculate the chi-squared image) and thus make the method more operational for semi-automatic map vector database update based on true orthophotos.

6. use of higher radiometric resolution data,

7. use of data including the infra-red spectral band, and

8. use of height data (dsm).

References

E.P. Baltsavias. Object extraction and revision by image analysis using existing geodata and knowledge: current status and steps towards operational systems. *ISPRS Journal of Photogrammetry and Remote Sensing*, 58(3-4):129–151, January 2004. ISSN 0924-2716. 3

Morton John Canty. *Image Analysis, Classification and Change Detection in Remote Sensing, With Algorithms for ENVI/IDL*. Taylor and Francis, CRC Press, second edition, 2010. ISBN 9781420087130. 6

Morton John Canty and Allan Aasbjerg Nielsen. Automatic radiometric normalization of multitemporal satellite imagery with the iteratively re-weighted MAD transformation. *Remote Sensing of Environment*, 112(3): 1025–1036, 2008. 4

EuroSDR. EuroSDR official publication no. 50, November 2006. 3

EuroSDR. EuroSDR official publication no. 56, December 2009. 3

Thomas Knudsen and Brian Pilemann Olsen. Automated change detection for updates of digital map databases. *Photogrammetric Engineering & Remote Sensing*, 69(11):1289–1296, November 2003. 3

Allan Aasbjerg Nielsen. The regularized iteratively reweighted MAD method for change detection in multi- and hyperspectral data. *IEEE Transactions on Image Processing*, 16(2):463–478, 2007. 4

Allan Aasbjerg Nielsen, Knut Conradsen, and James J. Simpson. Multivariate alteration detection (MAD) and MAF post-processing in multispectral, bi-temporal image data: New approaches to change detection studies. *Remote Sensing of Environment*, 64(1):1–19, 1998. 4.1

Brian Pilemann Olsen. *Maintenance of Digital Topographical Map Databases—Change Detection*. PhD thesis, Technical University of Denmark, Kort og Matrikelstyrelsen, Rentemestervej 8, DK-2400 København NV, Denmark, July 2004. 3

Brian Pilemann Olsen, Thomas Knudsen, and Poul Frederiksen. Digital change detection for map database update. In Jun Chen and Jie Jiang, editors, *Integrated Systems for Spatial Data Production, Custodian and Decision Support*, volume XXXIV (2), pages 357–363. ISPRS, August 2002. 3

Henning Skriver, Jesper Schou, and Wolfgang Dierking. Mapping by airborne synthetic aperture radar (SAR). In *International Archives of Photogrammetry and Remote Sensing*, volume XXXIII (B1), pages 307–312. ISPRS, July 2000. 3

A   Examples – time point pairs 2007/2009.

Figure 3: Example 1 for area from 6168_726. Changes between years 2007 and 2009. UL: The 2007 scene. UR: Change image. ML: Zoomed area from the 2007 scene. MR: Zoomed area from the 2009 scene. LL: Change image. LR: Significant change image.

Figure 4: Example 2 for area from 6168_726. Changes between years 2007 and 2009. UL: The 2007 scene. UR: Change image. ML: Zoomed area from the 2007 scene. MR: Zoomed area from the 2009 scene. LL: Change image. LR: Significant change image.
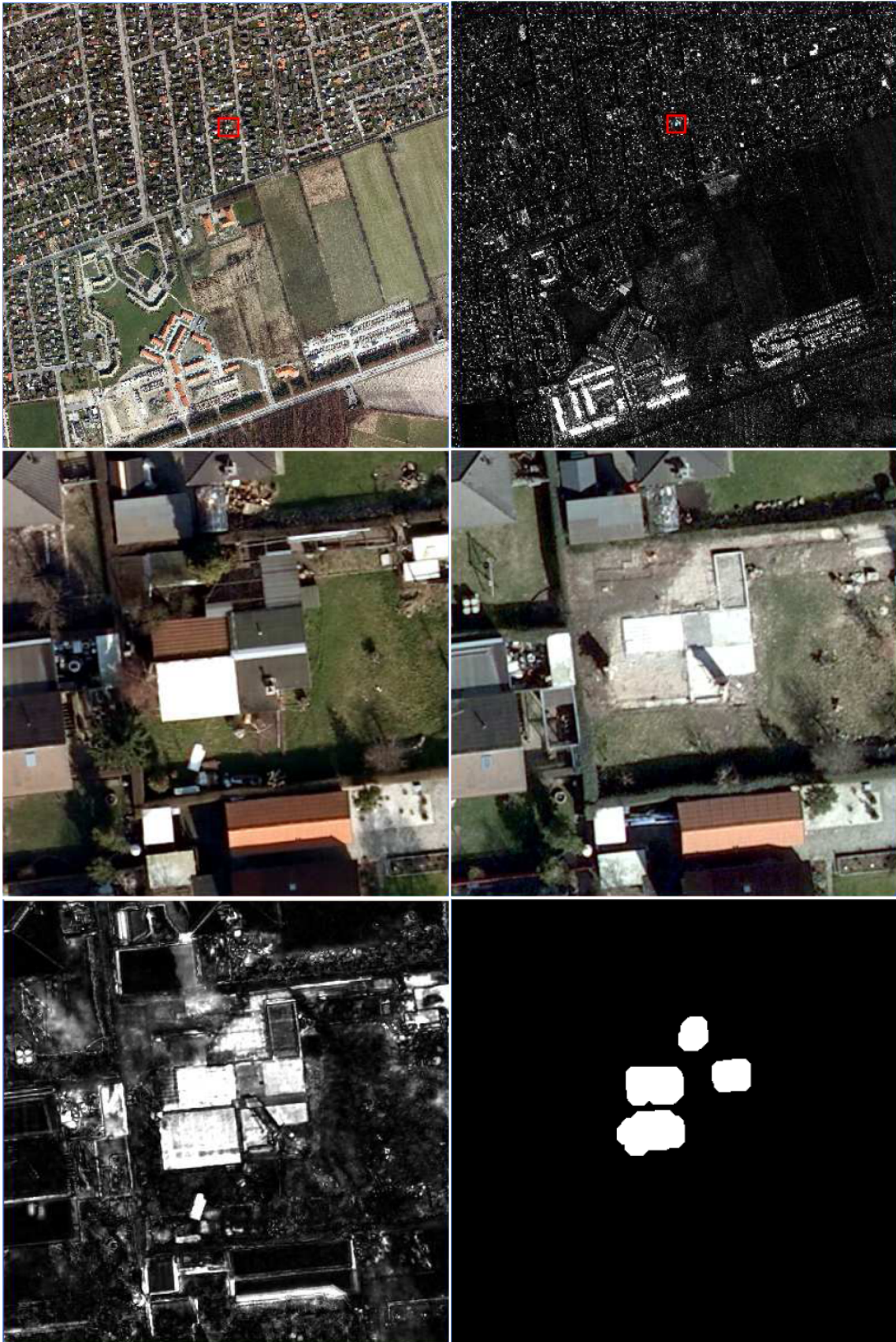
Figure 5: Example 3 for area from 6168_726. Changes between years 2007 and 2009. UL: The 2007 scene. UR: Change image. ML: Zoomed area from the 2007 scene. MR: Zoomed area from the 2009 scene. LL: Change image. LR: Significant change image.
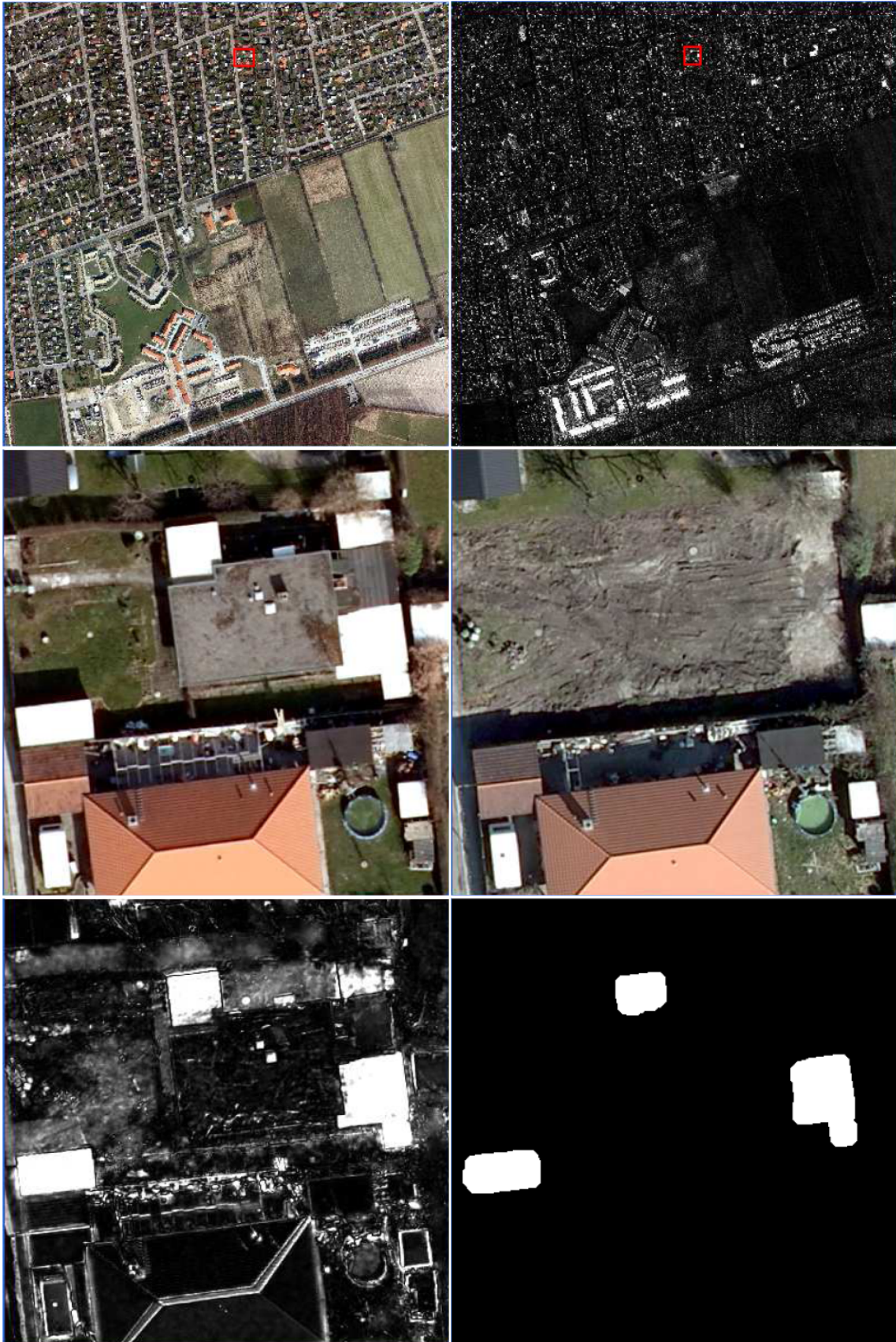
Figure 6: Example 4 for area from 6168_726. Changes between years 2007 and 2009. UL: The 2007 scene. UR: Change image. ML: Zoomed area from the 2007 scene. MR: Zoomed area from the 2009 scene. LL: Change image. LR: Significant change image.
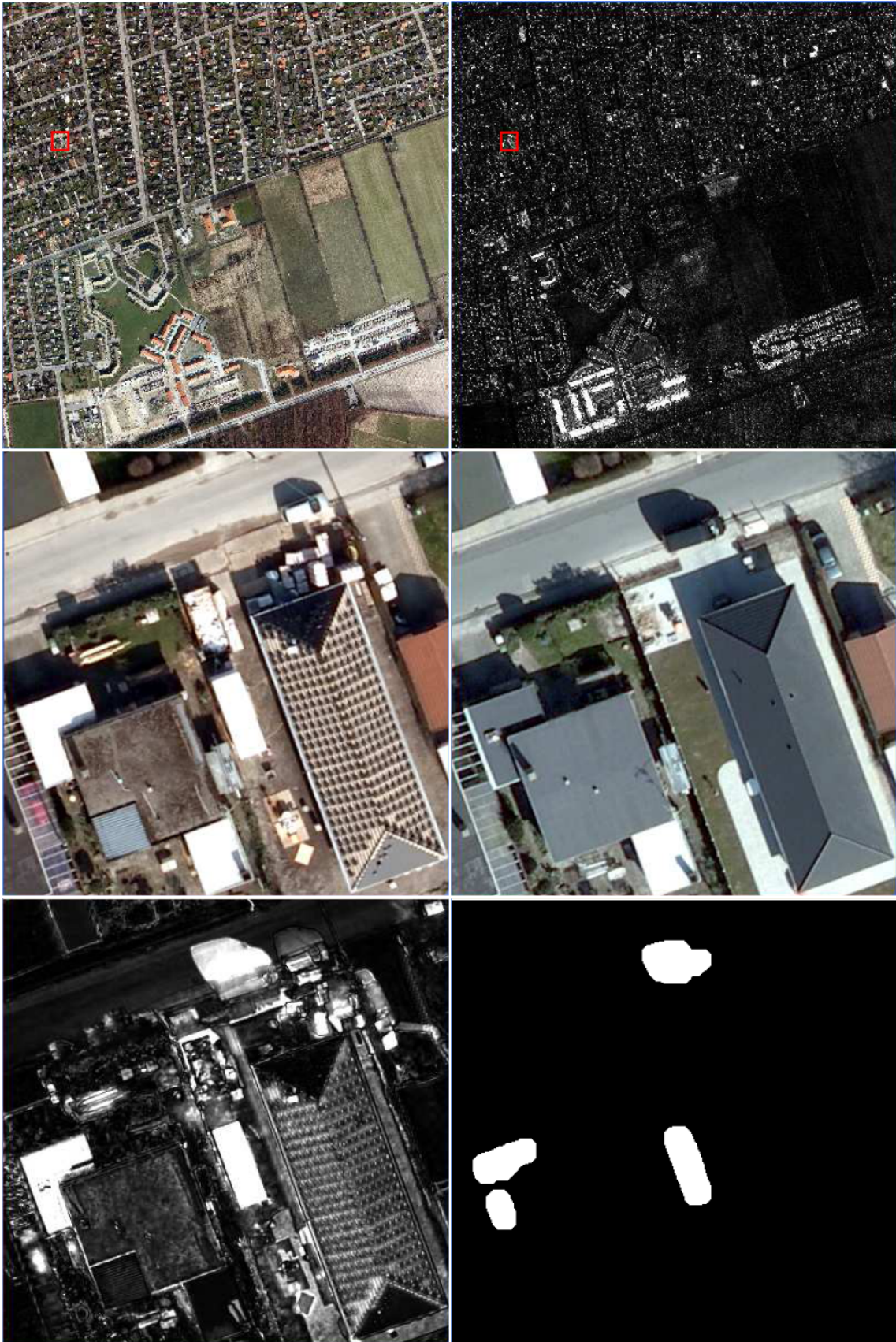
Figure 7: Example 5 for area from 6168_726. Changes between years 2007 and 2009. UL: The 2007 scene. UR: Change image. ML: Zoomed area from the 2007 scene. MR: Zoomed area from the 2009 scene. LL: Change image. LR: Significant change image.

Figure 8: Example 6 for area from 6168_726. Changes between years 2007 and 2009. UL: The 2007 scene. UR: Change image. ML: Zoomed area from the 2007 scene. MR: Zoomed area from the 2009 scene. LL: Change image. LR: Significant change image.
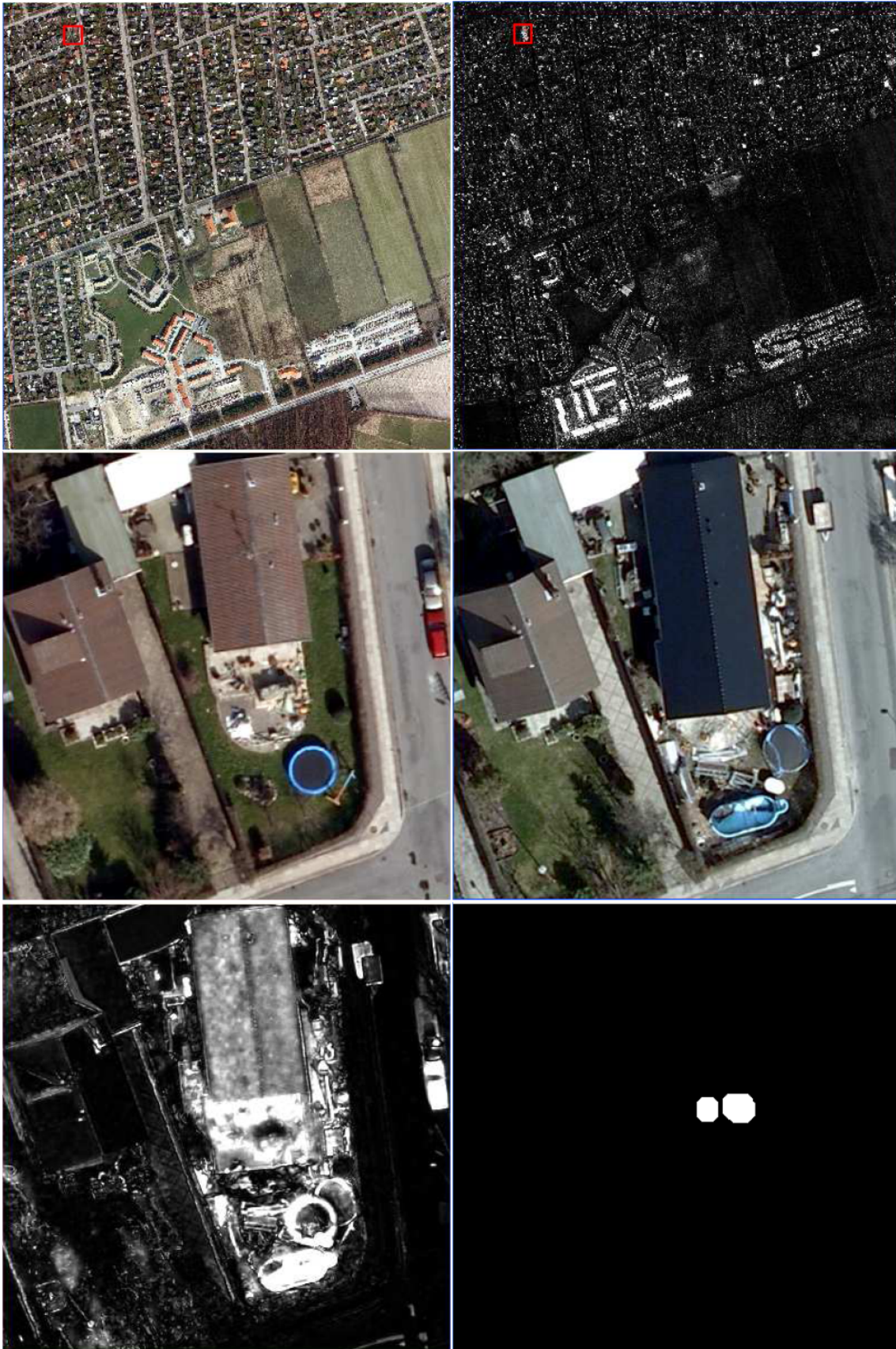
Figure 9: Example 7 for area from 6168_726. Changes between years 2007 and 2009. UL: The 2007 scene. UR: Change image. ML: Zoomed area from the 2007 scene. MR: Zoomed area from the 2009 scene. LL: Change image. LR: Significant change image.
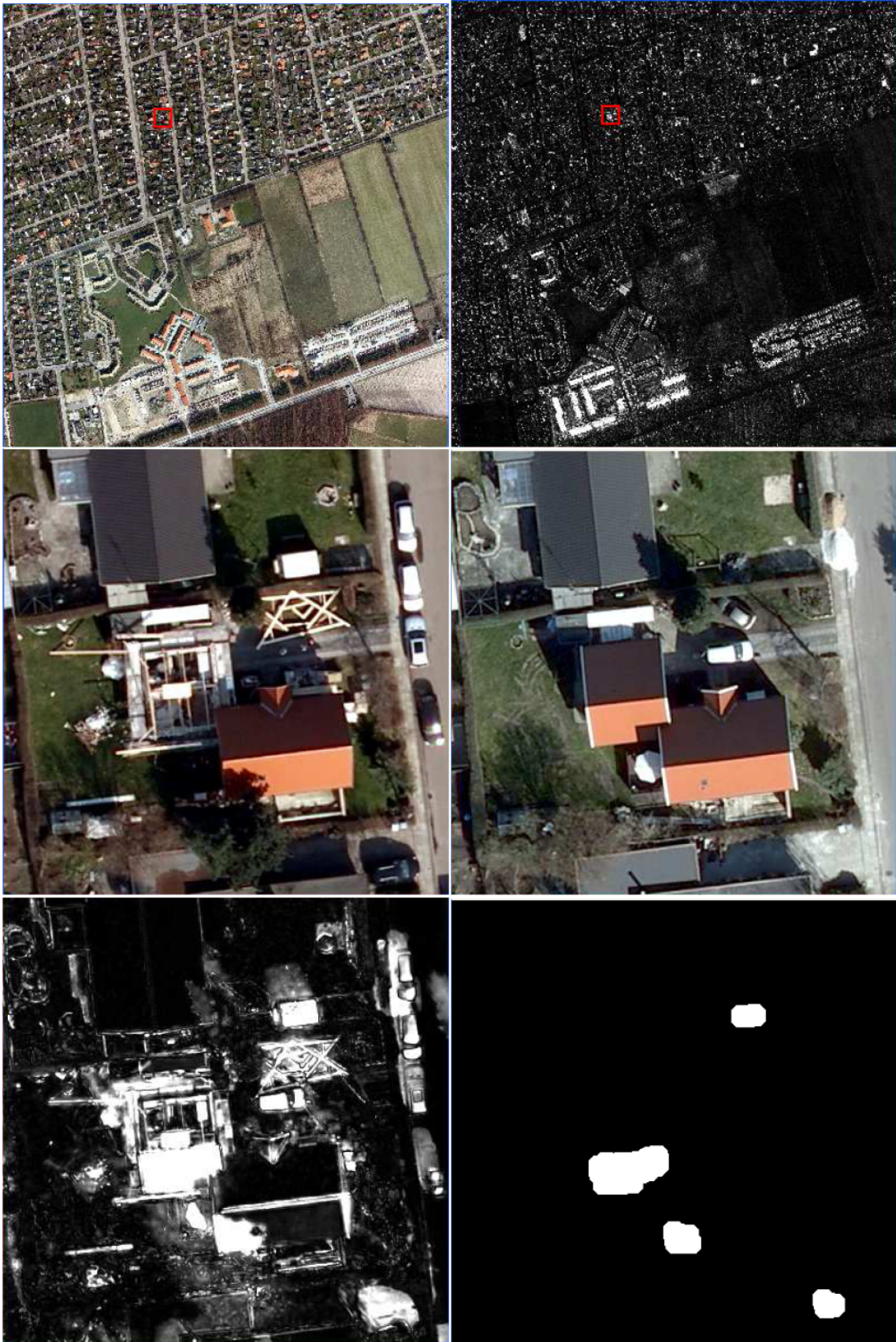
Figure 10: Example 8 for area from 6168_726. Changes between years 2007 and 2009. UL: The 2007 scene. UR: Change image. ML: Zoomed area from the 2007 scene. MR: Zoomed area from the 2009 scene. LL: Change image. LR: Significant change image.

Figure 11: Example 9 for area from 6168_726. Changes between years 2007 and 2009. UL: The 2007 scene. UR: Change image. ML: Zoomed area from the 2007 scene. MR: Zoomed area from the 2009 scene. LL: Change image. LR: Significant change image.

B Examples – registration problems, time point pairs 2007/2008.

For time point pairs 2007/2008, no thresholded and opened chi-squared images or "significant change images" are shown. All red squares and zooms for each example are linked so that they cover the same spatial region.

Figure 12: Example of registration problems. Changes between years 2007 and 2008. UL: The 2007 scene. UR: The 2008 scene. ML: Zoomed area from the 2007 scene. MR: Zoomed area from the 2008 scene. LL: Full scene change image. LR: Zoomed area change image.

C   Examples – registration problems, time point pairs 2008/2009.

For time point pairs 2008/2009, no thresholded and opened chi-squared images or "significant change images" are shown. All red squares and zooms for each example are linked so that they cover the same spatial region.

Figure 13: Example of registration problems. Changes between years 2008 and 2009. UL: The 2007 scene. UR: The 2008 scene. ML: Zoomed area from the 2007 scene. MR: Zoomed area from the 2008 scene. LL: Full scene change image. LR: Zoomed area change image.

MOLS BJERGE

Agri   137
      Agri Baunehøj

132
        44

Trehøje
(Dyrehøje)
127

Viderup
111
    41

Fuglsø

mS
                  3₂
         9₁
                  KOLSKÆR GRUND
              2₈
         7₃   R
                     12₁ (1.4.-15.11.)
                          BRB
         EGSMARK GRUND
11₄   7₄
12₁   2₂   5
        R'   PIKKELGRUND
12₆   7₁   6   5

Bogens Hoved
R   Cy
              0₆   6
     4₂   6
22   6   0₃ G
14₂

Egsmark

Dråby
Karls
. 53

9₂

3₁
4₃
G   R   OSp
18 Fl.G.5s   Fl.R.5s
3 PLADEN

Skelhøj
. 61
EBELTOFT
Havn 4,5m